

RESEARCH ARTICLE

G. Williams-Jones · J. Stix · M. Heiligmann
 A. Charland · B. Sherwood Lollar · N. Arner
 G. Garzón V. · J. Barquero · E. Fernandez

A model of diffuse degassing at three subduction-related volcanoes

Received: 16 December 1997 / Accepted: 27 January 2000

Abstract Radon, CO₂ and δ¹³C in soil gas were measured at three active subduction-related stratovolcanoes (Arenal and Poás, Costa Rica; Galeras, Colombia). In general, Rn, CO₂ and δ¹³C values are higher on the lower flanks of the volcanoes, except near fumaroles in the active craters. The upper flanks of these volcanoes have low Rn concentrations and light δ¹³C values. These observations suggest that diffuse degassing of magmatic gas on the upper flanks of these volcanoes is negligible and that more magmatic degassing occurs on the lower flanks where major faults and

greater fracturing in the older lavas can channel magmatic gases to the surface. These results are in contrast to findings for Mount Etna where a broad halo of magmatic CO₂ has been postulated to exist over much of the edifice. Differences in radon levels among the three volcanoes studied here may result from differences in age, the degree of fracturing and faulting, regional structures or the level of hydrothermal activity. Volcanoes, such as those studied here, act as plugs in the continental crust, focusing magmatic degassing towards crater fumaroles, faults and the fractured lower flanks.

Editorial responsibility: C. Newhall

Glyn Williams-Jones (✉) · John Stix
 Département de Géologie, Université de Montréal, Montréal,
 Québec, H3C 3J7, Canada
 e-mail: g.williams-jones@open.ac.uk
 Tel.: +44-1908-659023
 Fax: +44-1908-655151

Martin Heiligmann
 Department of Earth and Planetary Sciences, McGill University,
 Montréal, Québec, H3A 2A7, Canada

Anne Charland
 Falconbridge Ltd., 3296 Francis-Hugues Avenue, Laval, Québec,
 H7L 5A7, Canada

Barbara Sherwood Lollar · Neil Arner
 Department of Geology, University of Toronto, Toronto,
 Ontario, M5S 3B1, Canada

Gustavo Garzón V.
 INGEOMINAS, Observatorio Volcanológico y Sismológico,
 Pasto, A.A. 1795, Pasto, Colombia

Jorge Barquero · Erik Fernandez
 Observatorio Volcanológico y Sismológico de Costa Rica,
 Universidad Nacional, Apartado 86-3000, Heredia, Costa Rica

Present addresses:

Glyn Williams-Jones, Department of Earth Sciences,
 The Open University, Walton Hall, Milton Keynes, MK7 6AA,
 UK

John Stix, Department of Earth and Planetary Sciences,
 McGill University, Montréal, Québec, H3A 2A7, Canada

Key words Diffuse degassing · Radon · Carbon dioxide · Poás · Arenal · Galeras

Introduction

Until recently, it was believed that most gases emitted from a volcano were released from the main crater area. However, work by Allard et al. (1991), D'Alessandro et al. (1997), Giammanco et al. (1998) and others has shown that there may be significant degassing through the flanks of Mount Etna. While reactive gases, such as SO₂ and HCl, are released from the crater, along with significant amounts of H₂O and CO₂, flank degassing releases non-reactive gases such as CO₂, He and Rn. The study of flank degassing is important for gas budgets of volcanoes and for monitoring purposes. For example, flank degassing may release large quantities of CO₂ into the atmosphere, and changes in soil gas concentrations can sometimes be correlated with seismic and volcanic activity (cf. Baubron et al. 1991; Barberi and Carapezza 1994; Thomas et al. 1986; Heiligmann et al. 1997). The fundamental question is the following: Do most volcanoes emit significant quantities of gas from their flanks?

Soil gas concentrations may be affected by processes that cause stresses in the ground or change the pore spaces and volume of cracks and fissures. Proc-

esses such as (a) climatic variations (wind, rain, temperature and soil humidity), (b) atmospheric pressure variations, (c) deformation of a volcanic edifice, (d) volcanic and volcano-seismic activity, and (e) tectonic seismic activity all may have significant effects on soil gas concentrations (cf. King 1980; Shapiro et al. 1980; Schery and Petschek 1983; Hinkle 1990; Baubron et al. 1991; Badalamenti et al. 1993; Heiligmann et al. 1997; Giammanco et al. 1998).

The nature and development of the soil at various elevations on volcanoes may have a significant effect on the radon and CO₂ concentrations and on CO₂ flux values. At higher elevations, the soil often consists mainly of unconsolidated pyroclastic material, whereas the soils become progressively more developed at lower elevations as the amount of clay and organic material increases. The more developed soils are better able to retain moisture, which leads to increased sealing of the ground and subsequent build-up of gas. The less consolidated material will likely dry out faster after periods of precipitation, having efficiently removed the humidity by percolation. This allows the gas to escape relatively easily and enhances exchange with the atmosphere. The more organic-rich soils also may lead to increased concentrations of CO₂ due to the bacterial production of CO₂ and decomposition of organic material (Hinkle 1990). The temperature and vegetation type, which vary with altitude, also can have a significant effect on the rates of soil respiration and δ¹³C values. The upper flanks of the volcano also may act as recharge zones for groundwater, which transports soil gases to the lower flanks (James et al. 1999). Lastly, the thermal structure of the interior of the volcano may affect CO₂ fluxes, forcing magmatic gas up a relatively dry chimney rather than through the water-saturated flanks.

Geological setting

In order to investigate flank degassing, CO₂ and radon soil gases were studied on three subduction-related volcanoes. Arenal (1657 m) is an ~5-km-diameter stratovolcano situated in Costa Rica (10.46°N, 84.70°W), 90 km northwest of the capital, San José (Fig. 1). It has been in continuous activity since 1968, with frequent lava flows and strombolian–vulcanian eruptions (VEI=2–3). Poás (2708 m) is a stratovolcano ~14 km in diameter located approximately 35 km northwest of San José (10.20°N, 84.23°W) and is bordered by the Rio Saraquipi and Rio Toro faults (Fig. 2). The central crater, Laguna Caliente, has been active since the late 19th century. Central America is divided into seven tectonic segments mirrored by different styles of volcanism (Stoiber and Carr 1973). Arenal is situated ~80 km from the nearest segment break, whereas Poás lies ~40 km northwest of a segment break running through the Irazu-Turrialba vol-

canic complexes. Galeras (4200 m) is an ~25-km-diameter stratovolcano in southern Colombia (1.22°N, 77.37°W). The volcanic complex is intersected by the regional Romeral–Buesaco fault system that trends north–south (Fig. 3). Galeras also lies on a major tectonic break, the Guairapungo Fracture, which runs northwest–southeast through the northern Andes, and is intersected by the north/south-trending Interandean Valley (Hall and Wood 1985). Its most recent activity has been marked by explosive eruptions in May 1989, lava dome emplacement in late 1991 and six vulcanian eruptions in 1992–1993 (Stix et al. 1993, 1997).

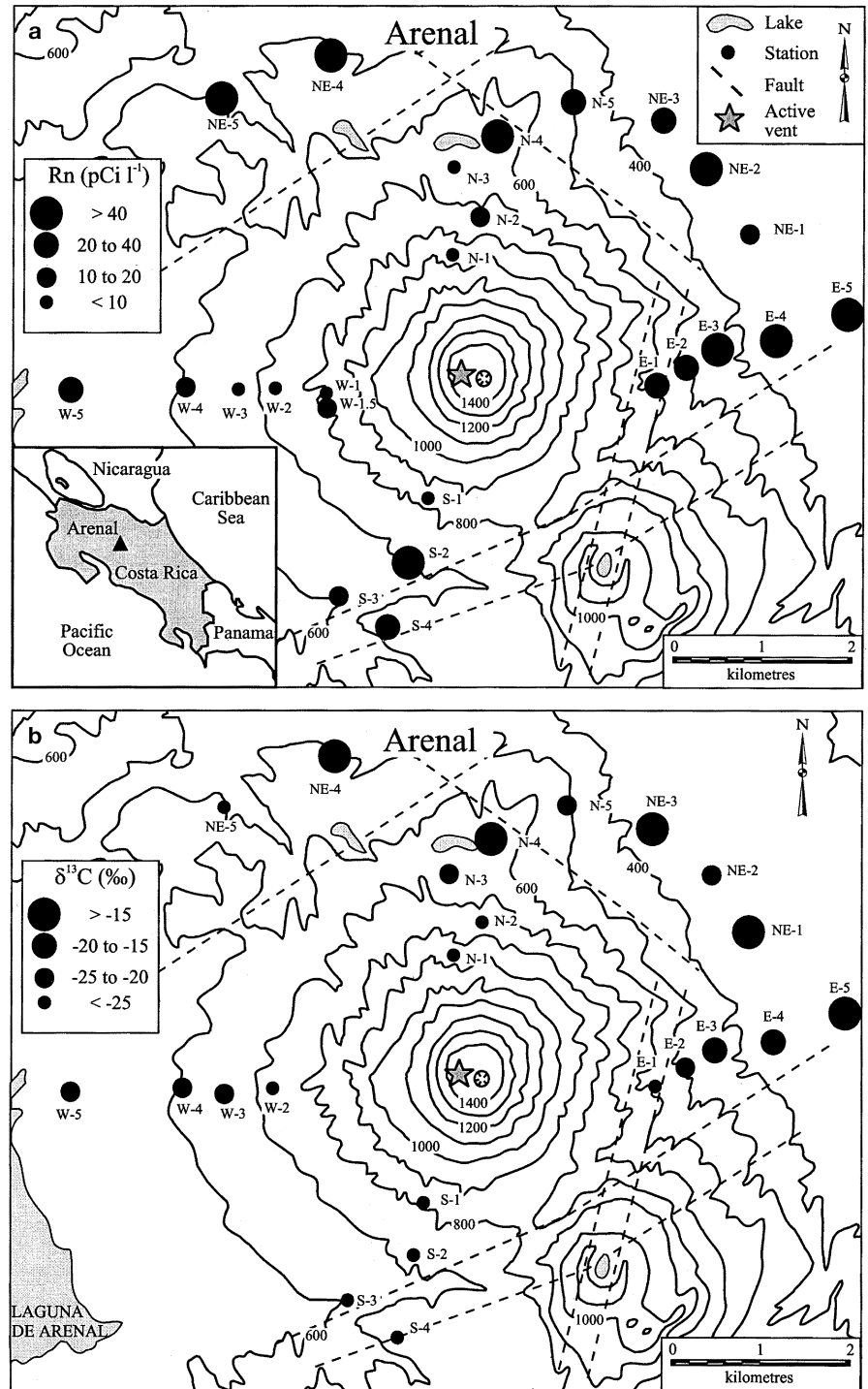
Methods

Diffuse degassing of Rn and CO₂ was studied at 25 representative stations on Arenal, 16 stations on Poás and 30 stations on Galeras, between 1993 and 1996 (Table 1; Charland et al. 1994; Heiligmann et al. 1997; Williams-Jones et al. 1997). Stations were chosen based on the geology, geographical location and, in the case of Galeras, their proximity to seismically active areas. Sampling was performed at approximately the same time every year (e.g., Arenal: March to April) in order to minimise any variations due to seasonal changes. The atmospheric pressure was measured at each station during each measurement and twice daily at reference base stations. No major pressure changes were observed during any of the field seasons. The measurement of soil gases was made in sealed tubes at a depth of ~75 cm where the impact of minor precipitation, pressure variation, wind turbulence and air exchange is limited.

²²²Rn was measured using the E-PERM technique developed by Rad-Elec Inc. (Kotrappa et al. 1988; Kotrappa and Stieff 1992) which consists of an electrostatically charged Teflon disk attached to an ion chamber of known volume. Two disks are placed at the top and bottom of a 1-m-long, 7.62-cm-diameter PVC tube sealed at the top and buried ~75 cm in the ground for a period of approximately 1 week. Results from the two disks were within 10%. The radioactive decay of radon in the chamber ionises the air, producing negative ions that contact the positively charged Teflon disk, resulting in a drop in voltage of the electret. Based on the voltage drop, chamber volume, exposure time and atmospheric pressure, the concentration of Rn can be calculated. On average, there was an uncertainty of ~10% of the value measured (see Appendix).

The ²²⁶radium-emanating potential of the ground was measured by taking soil samples from the bottom (~75 cm) of the ²²²Rn holes. These samples were kept in tightly sealed plastic bags in order to retain the soil humidity until they could be analysed. In the laboratory, 20–30 g of soil were placed in a ceramic petri dish and subsequently exposed to a short-term E-PERM electret in a sealed 3.74-l glass bottle for a

Fig. 1 Topographic map of Arenal volcano showing **a** average radon concentrations in pCi l^{-1} and **b** $\delta^{13}\text{C}$ values expressed as ‰. Contour interval is 100 m. *Star* represents the active vent; *dashed lines* represent possible faults mapped by Malavassi (1979) and Borgia et al. (1988)



period of 11 days. The radon-emanating potential of ^{226}Ra (RnERaC) then was calculated using the following formula (Rad Elec Inc. 1993):

$$\text{RnERaC} = \left(\frac{3.74 \cdot \frac{[\text{Rn}]}{M}}{1 - \frac{(1 - e^{-0.1813 \cdot \Delta t})}{0.1813 \cdot \Delta t}} \right) \cdot (1000) \quad (1)$$

where 3.74 is the volume (l) of the glass jar; $[\text{Rn}]$ is the ^{222}Rn concentration (pCi l^{-1}); M is the mass of soil (g) and Δt is the exposure time (days). The RnERaC, expressed in pCi kg^{-1} , represents the ability of the soil to produce radon gas. Thus, rather than a measure of ^{226}Ra concentration, the RnERaC is a measure of radon-emitting ^{226}Ra . This radon is typically produced near the edges of the soil grains, escaping into the pore spaces and subsequently travelling to the electret where it is measured.

Fig. 2 Topographic map of Poás volcano showing **a** average radon concentrations in pCi l^{-1} and **b** $\delta^{13}\text{C}$ values expressed as ‰. Contour interval is 500 m. *Star* represents the active vent, Laguna Caliente; *dashed lines* represent known faults; *dotted lines* represent the Inner and Outer calderas

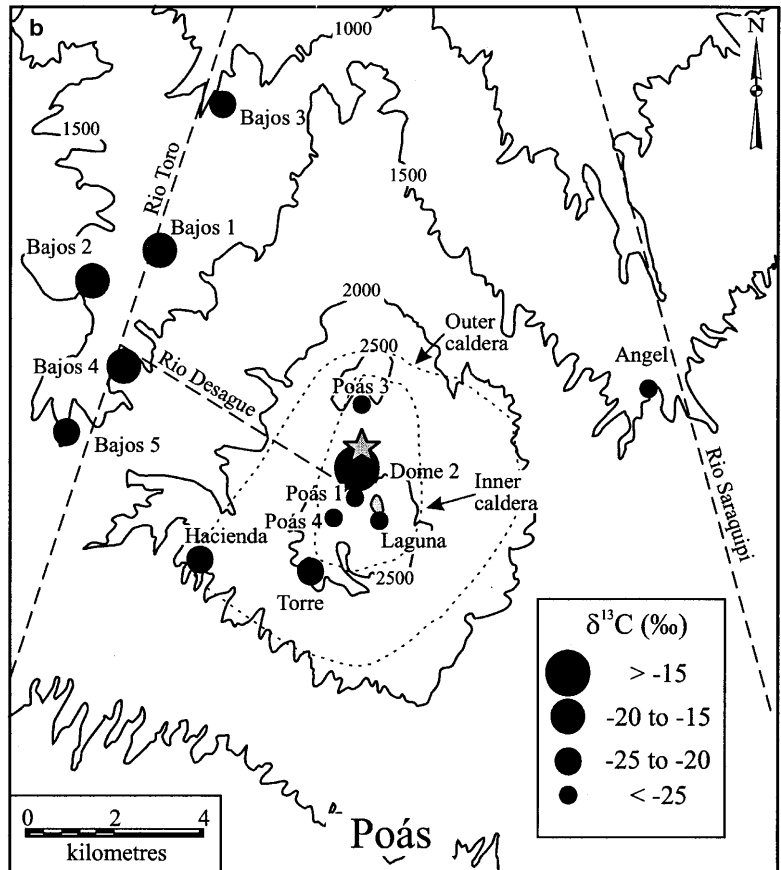
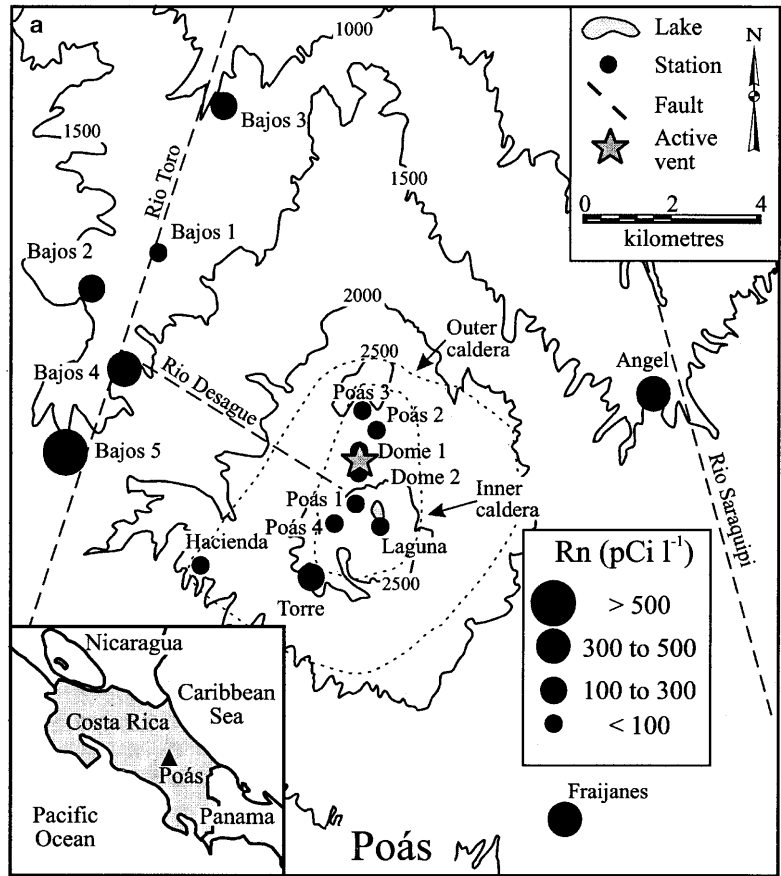
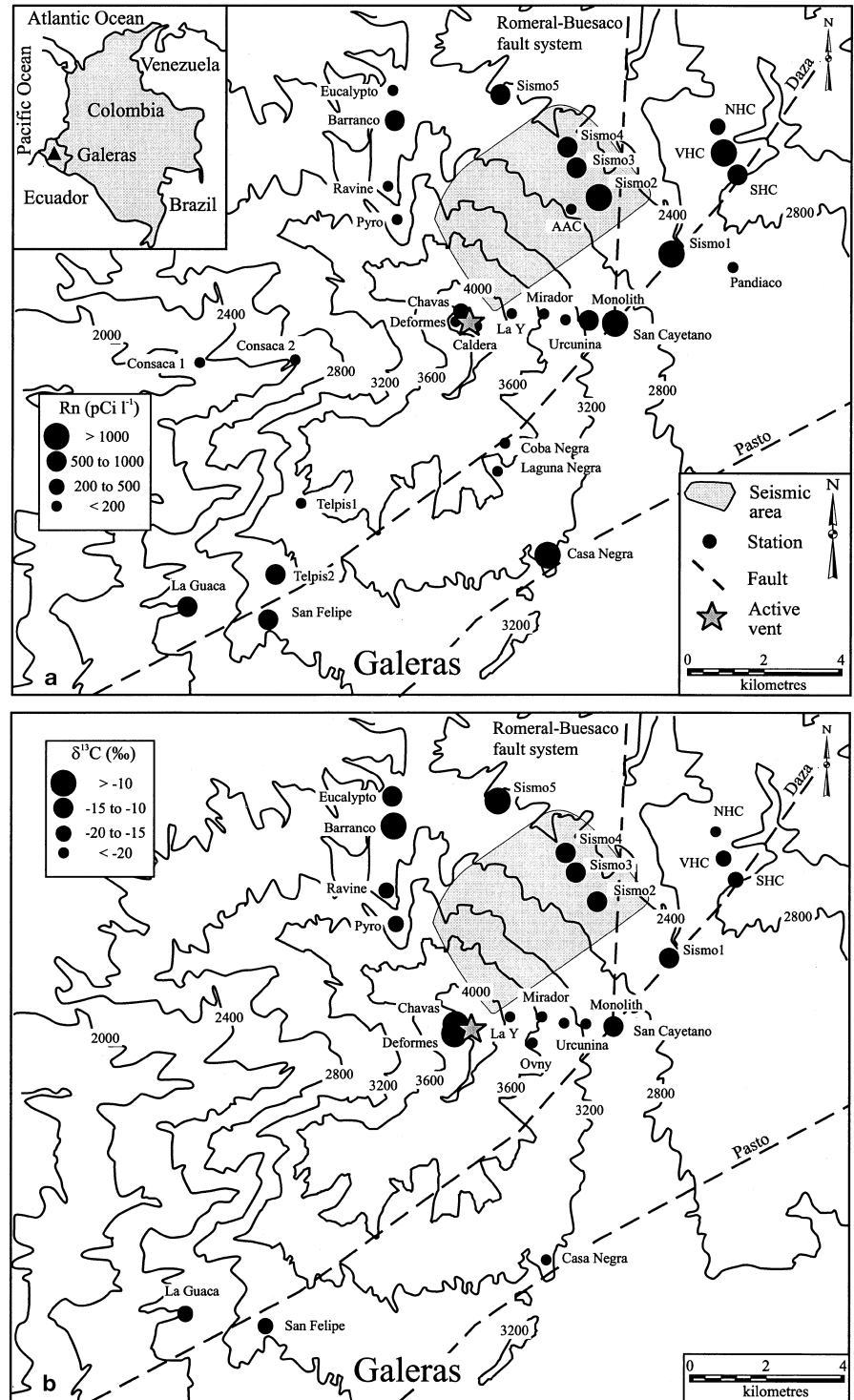


Fig. 3 Topographic map of Galeras volcano showing **a** average radon concentrations in pCi l^{-1} and **b** $\delta^{13}\text{C}$ values expressed as ‰. Contour interval is 400 m. *Shaded area* is an active seismic zone. *Star* represents the active vent. (After Heiligmann et al. 1997)



For CO_2 soil gas measurements, a 1-m-long, 1-cm-diameter aluminium tube, with five to six small perforations cut along the bottom 10 cm and sealed at the top, was placed next to the PVC tube to the same depth. CO_2 in the soil diffused into the tube, where it was measured periodically by an infrared gas analyser (ADC LFG-20 Landfill Gas Analyser). The gas analyser has a measurement range for CO_2 of 0–10 and 10–100 %, with corresponding precisions of 0.5 and

3 %, respectively. CO_2 concentrations were corrected for altitude using the following formula:

$$([\text{CO}_2]) \cdot (C_f), \quad (2)$$

where $[\text{CO}_2]$ is the volume percent CO_2 measured at the site and C_f is the correction factor calculated using:

$$C_f = 1 + (\Delta \text{Elev.}) \cdot (2.678 \times 10^{-4}), \quad (3)$$

Table 1 Average Rn, RnERaC, CO₂ and δ¹³C for Arenal, Poás and Galeras volcanoes

| Arenal | | | | | | | Poás | | | | | | | Galeras | | | | | | |
|---------|--------------|---------------------------|--------------------------------|--------------------------|-----------------------|-----------|--------------|---------------------------|--------------------------------|--------------------------|-----------------------|-----------|--------------|---------------------------|--------------------------------|--------------------------|-----------------------|--|--|--|
| Station | Field season | Rn (pCi l ⁻¹) | RnERaC (pCi kg ⁻¹) | CO ₂ (vol. %) | δ ¹³ C (‰) | Station | Field season | Rn (pCi l ⁻¹) | RnERaC (pCi kg ⁻¹) | CO ₂ (vol. %) | δ ¹³ C (‰) | Station | Field season | Rn (pCi l ⁻¹) | RnERaC (pCi kg ⁻¹) | CO ₂ (vol. %) | δ ¹³ C (‰) | | | |
| E-1 | 1995-1996 | 20 | 196 | 2.80 | -25.5 | Angel | 1994-1995 | 454 | 3.21 | -26.0 | AAC | 1993 | 73 | 0.7 | | | | | | |
| E-2 | 1995-1996 | 55 | 237 | 2.15 | -24.6 | Bajos 1 | 1994-1995 | 62 | 15.93 | -12.7 | Barranco | 1994 | 520 | 270 | 3.9 | | -8.7 | | | |
| E-3 | 1995-1996 | 42 | 263 | 6.44 | -19.6 | Bajos 2 | 1994-1995 | 229 | 5.81 | -13.8 | Caldera | 1994 | 10 | 0.0 | | | | | | |
| E-4 | 1995-1996 | 36 | 288 | 4.58 | -17.9 | Bajos 3 | 1994-1995 | 190 | 2.82 | -18.4 | Casa Negra | 1994 | 1030 | 250 | 2.5 | | -22.4 | | | |
| E-5 | 1995-1996 | 33 | 203 | 7.30 | -13.6 | Bajos 4 | 1994-1995 | 390 | 10.70 | -12.9 | Chavas | 1996 | 330 | | 16.2 | | -7.9 | | | |
| N-1 | 1995-1996 | 6 | 74 | 0.60 | -25.6 | Bajos 5 | 1994-1995 | 1150 | 5.30 | -15.3 | Coba Negra | 1994 | 86 | | 12.6 | | | | | |
| N-2 | 1995-1996 | 16 | 123 | 0.73 | -26.1 | Dome 1 | 1994-1995 | 7 | 0.01 | | Consaca 1 | 1994 | 150 | | 1.1 | | | | | |
| N-3 | 1995-1996 | 3 | 119 | 1.75 | -23.6 | Dome 2 | 1994-1995 | 19 | 0.71 | -6.2 | Consaca 2 | 1994 | 160 | 190 | 0.5 | | -8.7 | | | |
| N-4 | 1995-1996 | 41 | 192 | 7.15 | -14.3 | Hacienda | 1994-1995 | 36 | 2.58 | -19.5 | Deformes | 1995-1996 | 39 | | 0.5 | | | | | |
| N-5 | 1995-1996 | 36 | 205 | 3.37 | -23.9 | Laguna | 1994-1995 | 10 | 4.00 | -22.9 | Eucalypto | 1994 | 190 | | 3.5 | | -13.4 | | | |
| NE-1 | 1996 | 18 | 92 | 9.62 | -10.8 | Poas 1 | 1994-1995 | 8 | 2.95 | -24.7 | La Guaca | 1994 | 630 | 420 | 1.2 | | -17.9 | | | |
| NE-2 | 1996 | 63 | 101 | 2.86 | -22.7 | Poas 2 | 1994-1995 | 85 | 0.24 | | La Y | 1994 | 96 | 670 | 3.1 | | -22.7 | | | |
| NE-3 | 1996 | 37 | 103 | 7.53 | -15.0 | Poas 3 | 1994-1995 | 18 | 6.44 | -24.0 | Laguna Negra | 1994 | 28 | | 11.8 | | | | | |
| NE-4 | 1996 | 47 | 60 | 5.57 | -14.6 | Poas 4 | 1994-1995 | 41 | 2.96 | -22.8 | Mirador | 1994 | 110 | 120 | 2.1 | | -23.1 | | | |
| NE-5 | 1996 | 57 | 130 | 4.74 | -25.4 | Torre | 1994-1995 | 132 | 3.37 | -19.6 | Monolith | 1994 | 860 | 280 | 1.7 | | -21.1 | | | |
| S-1 | 1995-1996 | 8 | 104 | 0.96 | -30.4 | Fraijanes | 1994-1995 | 355 | 1.77 | | NHC | 1994 | 340 | 170 | 1.1 | | -20.2 | | | |
| S-2 | 1995-1996 | 41 | 142 | 6.98 | -26.1 | | | | | | Ovny | 1996 | | | | | -23.0 | | | |
| S-3 | 1995-1996 | 19 | 151 | 1.95 | -25.7 | | | | | | Pandiaco | 1993 | 95 | | 4.7 | | -19.4 | | | |
| S-4 | 1995-1996 | 32 | 180 | 2.61 | -25.6 | | | | | | Pyro | 1994 | 140 | 90 | 4.6 | | -18.3 | | | |
| W-1 | 1995-1996 | 8 | 109 | 0.04 | | | | | | | Ravine | 1994 | 140 | 130 | 3.6 | | -12.3 | | | |
| W-1.5 | 1995 | 10 | | | | | | | | | San Cayetano | 1994 | 1320 | 680 | 2.5 | | -18.7 | | | |
| W-2 | 1995-1996 | 7 | 280 | 1.13 | -25.3 | | | | | | San Felipe | 1994 | 960 | 780 | 0.8 | | -15.1 | | | |
| W-3 | 1995-1996 | 6 | 156 | 0.61 | -21.9 | | | | | | SHC | 1994 | 890 | 560 | 2.9 | | -14.2 | | | |
| W-4 | 1995-1996 | 13 | 155 | 0.95 | -20.9 | | | | | | Sismo 1 | 1995 | 1050 | 990 | 1.5 | | -11.4 | | | |
| W-5 | 1995-1996 | 27 | 180 | 7.85 | -20.7 | | | | | | Sismo 2 | 1995 | 1380 | 1020 | 1.6 | | -14.8 | | | |
| | | | | | | | | | | | Sismo 3 | 1995 | 810 | 1430 | 7.8 | | -14.2 | | | |
| | | | | | | | | | | | Sismo 4 | 1995 | 910 | 690 | 1.0 | | -8.5 | | | |
| | | | | | | | | | | | Sismo 5 | 1995 | 860 | 520 | 7.4 | | | | | |
| | | | | | | | | | | | Telpis 1 | 1994 | 100 | | 3.0 | | | | | |
| | | | | | | | | | | | Telpis 2 | 1994 | 600 | 360 | 1.3 | | -23.2 | | | |
| | | | | | | | | | | | Urcumina | 1994 | 90 | 90 | 2.5 | | -18.3 | | | |
| | | | | | | | | | | | VHC | 1994 | 1120 | 540 | 3.2 | | | | | |

The 1993-1995 Galeras data are from Heiligmann et al. (1997); 1996 Galeras data are from this article

where $\Delta\text{Elev.}$ is the difference in elevation in metres between the station and the base station, and 2.678×10^{-4} is a factor based on the linear regression of measurements of gas standards of known concentration taken at different elevations.

Diffuse CO_2 flux was measured using a technique developed by Moore and Roulet (1991). The technique consists of burying an inverted chamber ~ 75 cm in the ground. Tygon tubing from the top of the chamber allows for the measurement, by connection to the infrared gas analyser, of CO_2 concentrations over a period of 3–4 h. Measurements were taken every 15 min for the first 1.5 h and subsequently every 30 min for the remaining period. By plotting CO_2 concentration vs time and taking the slope of the initial linear segment of the curve, a flux measurement ($\text{mg m}^{-2} \text{s}^{-1}$) was calculated using the following formula:

$$Q_{\text{CO}_2} = \left(\frac{\Delta\text{CO}_2}{\Delta t} \right) \cdot \left(\frac{1}{M_{\text{air}}} \right) \cdot M_{\text{CO}_2} \cdot V \cdot \left(\frac{1}{A} \right) \cdot \delta_{\text{air}} \quad (4)$$

where ΔCO_2 is the difference between initial and final CO_2 concentrations (ppm); Δt is the elapsed time (s); M_{air} is the molecular weight of air ($2.8964 \times 10^{-2} \text{ kg mol}^{-1}$); M_{CO_2} is the molecular weight of CO_2 ($4.4010 \times 10^{-2} \text{ kg mol}^{-1}$); V is the chamber volume (14.9 m^3); A is the area of the chamber bottom (0.0519 m^2); and δ_{air} is the density of air (kg m^{-3}) calculated using $[(P/T) \cdot (3.483677 \times 10^{-6})]$ where P is the pressure in Pa and T is the temperature in degrees Kelvin.

Carbon isotope ($^{13}\text{C}/^{12}\text{C}$) analyses of CO_2 soil gases were performed at the University of Toronto using gas chromatograph–combustion–isotope ratio mass spectrometry (GC-C-IRMS). A 60-ml syringe was used to extract gases, which were then transferred into 25-ml stoppered, crimped vials that had been pre-evacuated and fixed with saturated mercuric chloride solution to prevent any isotopic changes due to bacterial activity during transport. Carbon isotope ratios are expressed as per mil (‰) deviation from Pee Dee Belemnite (PDB). Accuracy and reproducibility are both better than 0.5 ‰.

Results

Radon values differed substantially among the three volcanoes (Table 1), ranging from 3 to 63 pCi l^{-1} for Arenal (Fig. 1a), 7 to 1150 pCi l^{-1} for Poás (Fig. 2a) and 10 to 1380 pCi l^{-1} for Galeras (Fig. 3a). The values vary with the elevation and structure of the volcanoes (Fig. 4). At Arenal, radon concentrations increase towards the lower flanks (up to 63 pCi l^{-1} ; no data are available for the upper 600 m). Radon measurements on the E and S lines may be affected by possible faults on the eastern and southern flanks of the volcano (Fig. 1; Malavassi 1979; Borgia et al. 1988). Poás displays low values (e.g., Dome 1: 7 pCi

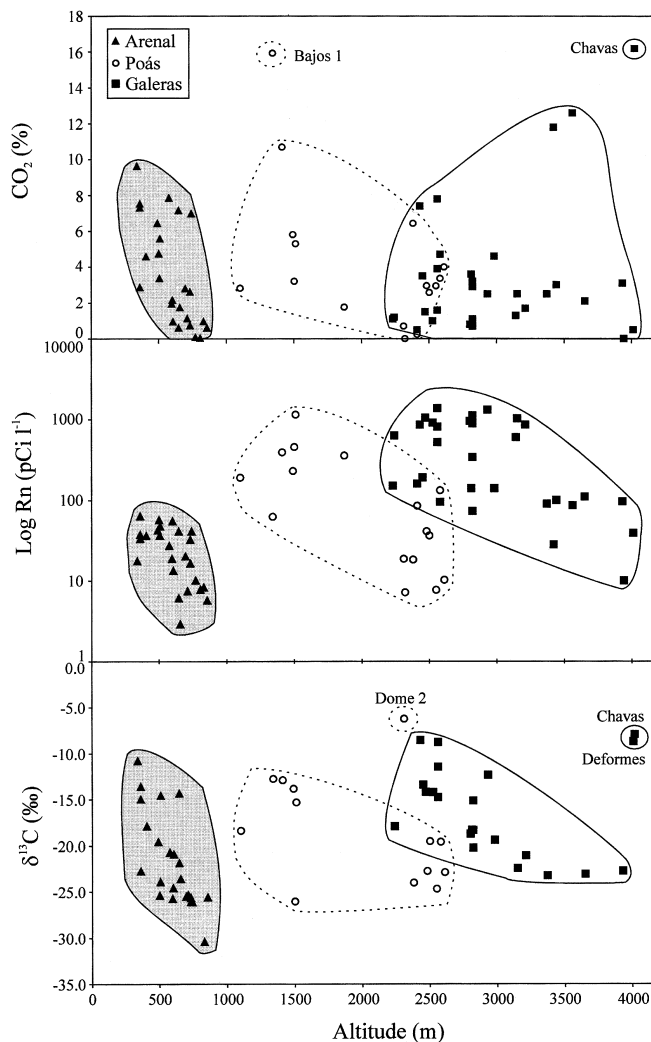


Fig. 4 CO_2 , Rn and $\delta^{13}\text{C}$ vs altitude for Arenal, Poás and Galeras volcanoes. Note the general negative correlations with radon and CO_2 decreasing and $\delta^{13}\text{C}$ becoming lighter with increased altitude except for sites nearest the active vents

l^{-1} to Torre: 130 pCi l^{-1}) in the vicinity of the active crater and higher values on its flanks (e.g., Fraijanes: 355 pCi l^{-1}) and near faults (e.g., Bajos stations: 60–1150 pCi l^{-1}). At Galeras, values also are high near faults and a zone north–northeast of the crater where swarms of high-frequency earthquakes were recorded in 1993 and 1995 (e.g., Barranco: 520 pCi l^{-1} to Sismo 2: 1380 pCi l^{-1} ; Fig. 3). High radon concentrations also were observed at one station near Chavas fumarole, located on the outer flanks of the active cone within the summit caldera ($\sim 330 \text{ pCi l}^{-1}$).

The ^{226}Ra -emanating potentials (RnERaC) on Arenal ranged from 60 to 288 pCi kg^{-1} , whereas values on Galeras varied from 90 to 1430 pCi kg^{-1} (Heiligmann et al. 1997). Typically, the RnERaC values are highest at stations with high radon (e.g., Arenal: E-2, E-3 and E-4; Galeras: Sismo 1, Sismo 2,

Sismo 3 and San Felipe) and lowest at stations with low radon concentrations (e.g., Arenal: W-1, N-1 and N-3; Galeras: Pyro, Urcunina, Mirador and Ravine; Table 1). No RnERaC data are available for Poás.

The CO₂ concentrations varied from 0.04 to 9.6 % at Arenal, <0.1 to 16 % at Poás and 0.0 to 16 % at Galeras (Table 1). On Arenal, the concentrations are generally low on the upper flanks (>700 m; 0.04–2.8 %) and higher on the lower flanks (<700 m; 0.95–9.6 %) and near possible faults (2.6–7.3 %). Station S-2 (740 m) has anomalously high CO₂ (6.98 %) due perhaps to its proximity to a possible fault. It is also near a stream which might suggest concentration of the gas beneath a water-saturated soil. At Poás, low CO₂ values are found in the inner caldera (0.01–3.4 %), and higher values are found on lower flanks at stations located near the Rio Toro fault (3.2–16 %). The anomalously high CO₂ concentrations at Laguna (4 %) and Poas 3 (6.4 %) also may be due to gas accumulation beneath an impermeable water-saturated soil. This contrasts with Galeras where CO₂ concentrations are more variable and commonly higher on the volcano (up to 13 %) than near faults (1.2–3.2 %; Heiligmann et al. 1997).

The δ¹³C values (Table 1) ranged from –10.8 to –30.4 ‰ at Arenal (Fig. 1b), –6.2 to –26.0 ‰ at Poás (Fig. 2b) and –8.5 to –23.2 ‰ at Galeras (Fig. 3b). On Arenal, δ¹³C values are generally heaviest on the lower flanks (<700 m; –10.8 to –25.7 ‰) and lighter at higher elevations (>700 m; –25.3 to –30.4 ‰; Fig. 4). Likewise, δ¹³C values at Poás are generally heavier on the lower flanks near the Rio Toro fault

zone (–12.7 to –18.4 ‰) than in the summit area, except for the Dome-2 station (–6.2 ‰, 1995 measurement), which is situated near fumaroles in the active crater (Table 1). It is noteworthy that the Dome 2 station had a δ¹³C value of –21.1 ‰ and CO₂ concentration of 0.02 % in 1994. The other summit stations at Poás all have δ¹³C values lighter than –19.5 ‰, suggesting that the magmatic component (–3 to –8 ‰) is absent or insignificant. At Galeras δ¹³C in CO₂ heavier than –15 ‰ is recorded near active crater fumaroles (e.g., Chavas: –7.9 ‰), and lower on the flanks near a seismically active zone (e.g., Sismo 5: –8.5 ‰).

Diffuse CO₂ flux values range from 0.04 to 3.37 mg m^{–2} s^{–1} on Arenal; 0.23 to 1.62 mg m^{–2} s^{–1} on Poás and 0.0 to 1.38 mg m^{–2} s^{–1} on Galeras (Table 2). The biogenic component of CO₂ flux varies greatly depending on soil type but is generally less than 0.12 mg m^{–2} s^{–1} in tropical forests such as those on Arenal, Poás and Galeras (cf. Dugas 1993; Fernandez et al. 1993; Pinol et al. 1995; Rahn et al. 1996; Janssens et al. 1998). A plot of CO₂ concentrations vs CO₂ flux shows a positive correlation to varying degrees depending on the volcano (Fig. 5).

An estimate of the flux of magmatic CO₂ on Galeras was made by Heiligmann (1996) with the following assumptions:

1. Deep CO₂ flux was observed only in the seismically active north–northeast zone and near the Romeral–Buesaco fault (a total affected area of 25 km²).
2. The CO₂ flux of Barranco station is representative for this region.

Table 2 Diffuse CO₂ flux for Arenal, Poás and Galeras volcanoes

| Arenal | | | Poás | | | Galeras | | |
|---------|---|-----------------------------|-----------|---|-----------------------------|--------------|---|-----------------------------|
| Station | CO ₂ flux (mg m ^{–2} s ^{–1}) | CO ₂ (vol. %) | Station | CO ₂ flux (mg m ^{–2} s ^{–1}) | CO ₂ (vol. %) | Station | CO ₂ flux (mg m ^{–2} s ^{–1}) | CO ₂ (vol. %) |
| E-2 | 0.11 | 2.03 | Poas 3 | 0.73 | 6.66 | Barranco | 0.64 | 2.9 |
| E-3 | 2.05 | 6.50 | Poas 3 | 0.74 | 6.66 | Caldera | 0.00 | 0.0 |
| E-4 | 1.11 | 5.00 | Poas 4 | 0.23 | 3.03 | Casa Negra | 1.16 | 2.5 |
| E-5 | 3.37 | 8.30 | Poas 4 | 0.24 | 3.03 | Coba Negra | 1.38 | 12.2 |
| N-2 | 0.03 | 0.55 | Poas 4 | 0.25 | 3.10 | Consaca 1 | 0.29 | 1.2 |
| N-4 | 0.93 | 5.60 | Poas 4 | 0.24 | 3.10 | Consaca 2 | 0.13 | 0.5 |
| S-1 | 0.08 | 0.72 | Hacienda | 0.80 | 3.41 | Eucalypto | 0.72 | 2.7 |
| S-2 | 0.55 | 8.00 | Hacienda | 0.98 | 3.41 | La Guaca | 0.17 | 0.8 |
| S-3 | 0.35 | 1.80 | Bajos 1 | 1.50 | 20.40 | Laguna Negra | 0.91 | 10.0 |
| W-2 | 0.43 | 0.84 | Bajos 1 | 1.62 | 20.40 | Mirador | 0.75 | 1.1 |
| W-3 | 0.10 | 0.69 | Bajos 3 | 0.25 | 2.63 | Monolith | 0.60 | 1.0 |
| W-5 | 0.42 | 7.15 | Bajos 3 | 0.27 | 2.63 | NHC | 0.24 | 0.8 |
| W-5 | 1.73 | 7.15 | Torre | 0.31 | 4.18 | Pyro | 0.59 | 5.6 |
| | | | Torre | 0.43 | 4.18 | Ravine | 0.81 | 6.4 |
| | | | Fraijanes | 0.37 | 2.00 | San Cayetano | 0.28 | 2.2 |
| | | | Fraijanes | 0.37 | 2.00 | San Felipe | 0.11 | 0.7 |
| | | | | | | SHC | 0.34 | 2.7 |
| | | | | | | Telpis 1 | 0.36 | 1.9 |
| | | | | | | Telpis 2 | 0.22 | 0.9 |
| | | | | | | Urcunina | 1.32 | 1.7 |
| | | | | | | VHC | 0.44 | 2.6 |

Arenal data from 1995; Poás data from 1994; Galeras data from 1994 (Heiligmann 1996)
CO₂ concentrations are those measured at the time of flux measurement

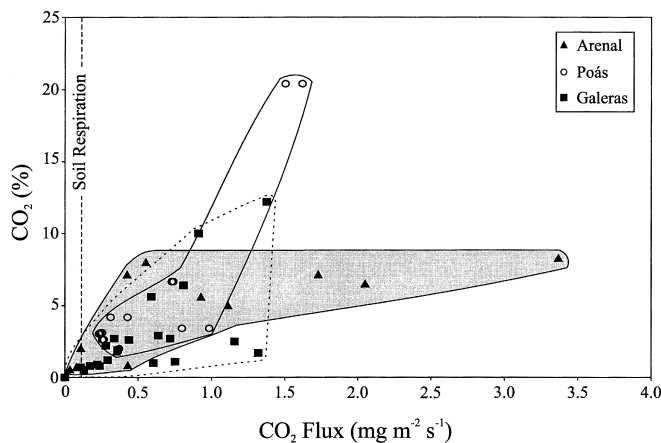


Fig. 5 CO_2 concentration vs CO_2 flux for Arenal, Poás and Galeras volcanoes. Correlation coefficients are 0.71, 0.89 and 0.64 for Arenal, Poás and Galeras, respectively. Dashed line represents the typical biogenic component of CO_2 flux ($<0.12 \text{ mg m}^{-2} \text{ s}^{-1}$)

3. Only biogenic (i.e., $\delta^{13}\text{C} \sim 23\text{‰}$) and deep carbon (i.e., $\delta^{13}\text{C} \sim 6\text{‰}$) were present in the CO_2 soil gas.
4. The average deep carbon contribution for this region was 50%.

Thus, for a 25 km^2 area with a diffuse CO_2 flux of $0.63 \text{ mg m}^{-2} \text{ s}^{-1}$ (Table 2), there is a total flux 1370 tonnes per day (t d^{-1}). If 50% of the total flux is magmatic in origin, then 690 t d^{-1} ($5.7 \times 10^9 \text{ mol year}^{-1}$) of deep CO_2 degassed passively from the volcano. According to Heiligmann (1996), all other flank areas on Galeras show no significant magmatic CO_2 component.

Discussion

High radon concentrations in soil gases on these and many other volcanoes are often associated with faults and areas of seismic activity (Crenshaw et al. 1982; Gasparini and Mantovani 1978; Thomas et al. 1986; Connor et al. 1996; Heiligmann et al. 1997). For example, on the lower flanks of Galeras, stations near the Pasto (e.g., SHC, VHC) and Daza faults (e.g., Casa Negra) have high radon concentrations, possibly the result of fracturing at shallow levels and/or advective transport along the fault zone which may suggest relatively high permeabilities. However, the slow transport velocities and short half-life of radon suggest that deep radon probably does not reach the surface directly. On these three volcanoes, high radon values are more typically associated with soil development at lower elevations, as shown by the high radon-emanating potentials of the soil at Arenal and Galeras (Table 1). For example, on Arenal, station S-1 has an RnERaC of 104 pCi kg^{-1} and an average radon concentration of 8 pCi l^{-1} , whereas S-4 has an RnERaC of 180 pCi kg^{-1} and an average radon value of 32 pCi l^{-1}

l^{-1} (Table 1). Similar trends are observed on the N line where N-1 has an RnERaC of 74 pCi kg^{-1} and radon concentration of 6 pCi l^{-1} , whereas N-5 has an RnERaC of 205 pCi kg^{-1} and an average radon value of 36 pCi l^{-1} (Table 1). On Galeras, the initially good correlation between Rn concentration and $\delta^{13}\text{C}$ disappears when radon is normalised by the RnERaC (Fig. 6). This suggests that the radon-emanating potential of the soil is in large part responsible for measured radon values. Thus, although superficial faulting and fracturing may increase radon concentrations to some extent, the radon soil gas is essentially surficial.

It has been suggested that Mount Etna is covered by a halo of magmatic CO_2 from crater and flank degassing, especially concentrated near faults and radial dykes (Allard et al. 1991), with heavy $\delta^{13}\text{C}$ values along these structures and at lower elevations interpreted as being due to the influence of marine carbonates. Allard et al. (1991) indicate that CO_2 degassing from Mount Etna's flanks may be comparable in magnitude to that released from the crater area ($0.3 \times 10^{12} \text{ mol year}^{-1}$). However, our observations on Arenal, Poás and Galeras indicate that there is no significant magmatic CO_2 being released diffusely on the upper flanks of these volcanoes. Recent studies on other volcanoes show similar spatial patterns of CO_2 release. Work on Oldoinyo Lengai (Brantley and Koe-

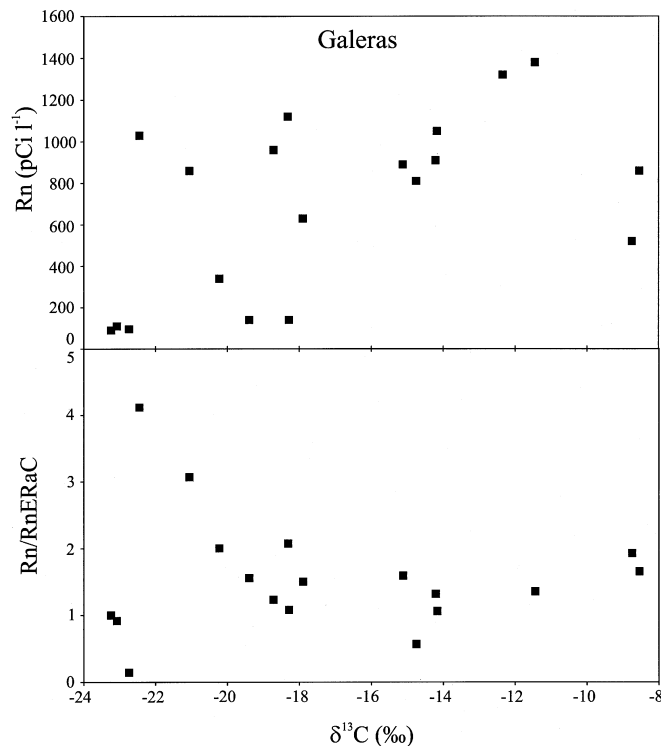


Fig. 6 Radon vs $\delta^{13}\text{C}$ and Rn/RnERaC vs $\delta^{13}\text{C}$ for Galeras volcano. Excluding three outliers (Casa Negra, Barranco and Sismo 5), the correlation coefficient of Rn vs $\delta^{13}\text{C}$ is 0.8. However, when radon is normalised by the radon emanating potential (RnERaC), the correlation coefficient is only 0.003. (Modified after Heiligmann et al. 1997)

penick 1995) has shown that $\sim 75\%$ of the CO_2 flux comes from seven crater vents, with less than 2% of the total flux from the flanks (Koepenick et al. 1996). At Mount Shasta and Three Sisters volcanoes in the Cascades, the presence of ^{14}C -rich waters from alpine creeks implies that little magmatic CO_2 escapes from the upper slopes of these volcanoes (Rose and Davison 1996). Near Mammoth Mountain on the southwestern margin of Long Valley Caldera, areas of diffuse CO_2 degassing observed since 1990 (Farrar et al. 1995; Rahn et al. 1996; Gerlach et al. 1998) are located on the periphery of the mountain and appear to be associated with north- and northwest-trending faults. New work on Mount Etna now suggests that levels of CO_2 flank degassing may in fact have been overestimated (D'Alessandro et al. 1997; Allard 1998). According to these workers, the rate of diffuse CO_2 degassing from soils on Mount Etna ranges from 0.023 to $0.11 \times 10^{12} \text{ mol year}^{-1}$, up to an order of magnitude less than that estimated by Allard et al. (1991). Nevertheless, this is still at least four times greater than the diffuse CO_2 flux ($5.7 \times 10^9 \text{ mol year}^{-1}$) calculated for Galeras by Heiligmann (1996).

Although soil respiration in the tropics ($<0.12 \text{ mg m}^{-2} \text{ s}^{-1}$) may be responsible for some of the observed CO_2 flux, values ranging up to $3.37 \text{ mg m}^{-2} \text{ s}^{-1}$ (Table 2) clearly suggest that a magmatic component is also important. Furthermore, at Arenal and Poás (excluding the Dome 2 sample), $\delta^{13}\text{C}$ values heavier than -15‰ are found only at stations with CO_2 concentrations $>5\%$, and these stations are located mainly on the lower flanks (Fig. 7). Summit stations on Poás (Dome 2) and Galeras (Deformes, Chavas), which are located near actively venting fumaroles, clearly show a magmatic signature. This inverse correlation would certainly not be expected if only organic CO_2 was present.

The Dome 2 station on Poás showed a marked change between 1994 and 1995 with CO_2 concentrations increasing from 0.01 to 2.1% and $\delta^{13}\text{C}$ values increasing from -21.1 to -6.2‰ . This suggests that the permeability of the crater area may play a role in facilitating or hindering the flow of magmatic gas. Furthermore, the 1994 data for this station suggest that the system may be able to efficiently seal itself. This may also explain the relatively high CO_2 concentrations at Poas 3 and Laguna. Lower permeability in a water-saturated soil (perhaps induced by precipitation) may inhibit CO_2 flux, causing it to concentrate beneath the surface.

An alternative hypothesis to our model is that the upper flanks of the volcanoes are actually permeable, resulting in low CO_2 values. However, if magmatic CO_2 were being transported to the surface through the upper flanks, we would expect to see comparatively heavy carbon isotope values. Yet the values from the upper slopes are generally light, indicating that the magmatic component is small (Fig. 4). A second alternative hypothesis is that groundwaters flush

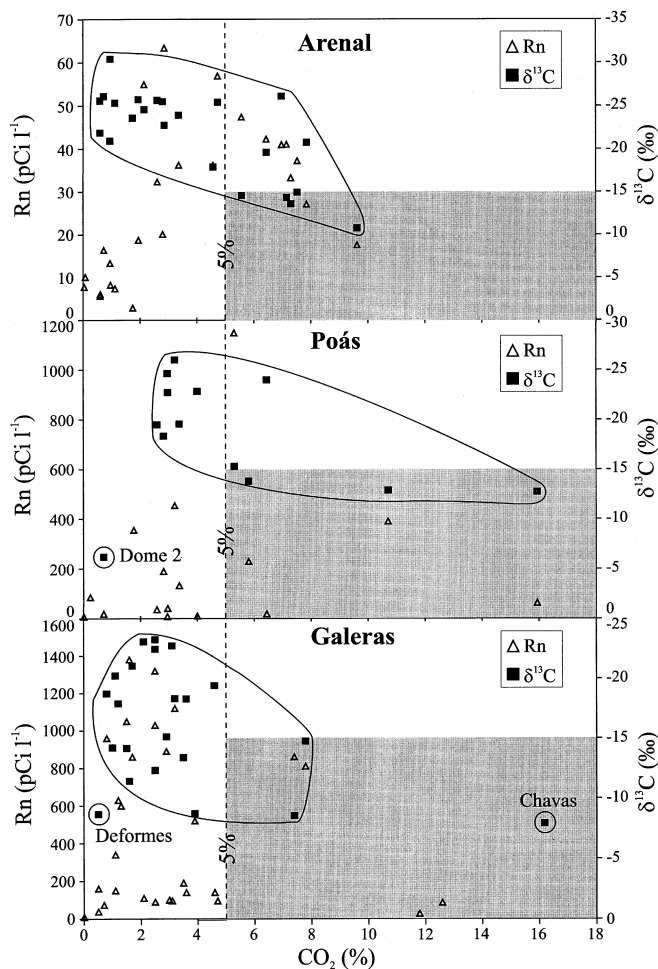


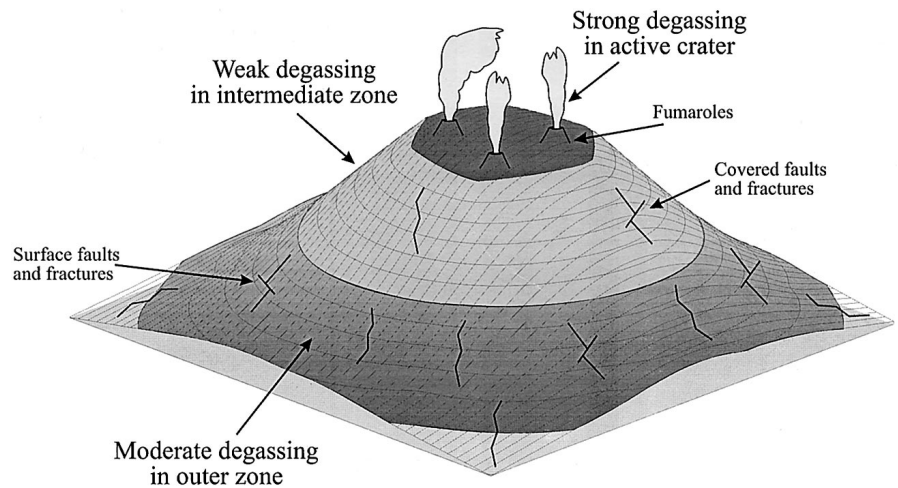
Fig. 7 Radon and $\delta^{13}\text{C}$ vs CO_2 concentration for Arenal, Poás and Galeras volcanoes. For Arenal and Poás, stations with heavy $\delta^{13}\text{C}$ ($>-15\text{‰}$) have high CO_2 ($>5\%$), whereas at Galeras, stations with light $\delta^{13}\text{C}$ ($<-15\text{‰}$) have low CO_2

magmatic gas from the upper flanks to lower altitudes at Poás and Arenal, resulting in higher CO_2 contents in soil gas at lower elevations. This is a plausible hypothesis that may play an additional role in mobilising gas and concentrating it on the lower slopes of the volcanoes.

Why does Arenal have significantly lower Rn values than Galeras and Poás? We propose three possible explanations:

1. Arenal is less than 3000 years old (Borgia et al. 1988), whereas Poás is $\sim 1 \text{ Ma}$ (Prosser and Carr 1987) and Galeras is $>1.1 \text{ Ma}$ (Calvache et al. 1997). Owing to its youth, Arenal is less fractured and faulted than Poás and Galeras, resulting in less surface area for radon production.
2. The older fractured edifices of Galeras and Poás also have more mature hydrothermal systems (Rowe et al. 1995; Fischer et al. 1997), which may help in mobilising radon-parent elements such as Ra and U.

Fig. 8 Diagram of a stratovolcano shows concentric zoning of gas flow. Strong degassing occurs in the active crater area, weak degassing on the upper flanks, and renewed degassing in a fractured outer zone



3. Large regional structures also may have an effect in controlling surficial radon distributions. Arenal is almost 80 km from the nearest segment break, whereas both Poás and Galeras lie on important regional fault systems. These major structures may thus facilitate the transport and remobilisation of the parental isotope radium from wall-rock and hydrothermal sources and result in elevated Rn concentrations.

Conclusion

The three factors discussed previously – fracturing, hydrothermal development and regional structure – may affect flank degassing to variable degrees. The radon and $\delta^{13}\text{C}$ evidence presented here suggest that diffuse gases are unable to penetrate the upper flanks of these volcanoes, either because the young lavas are not sufficiently permeable or sufficiently faulted that outgassing can be focused, or because groundwater recharge through the upper slopes absorbs and transports the magmatic CO_2 . We propose that stratovolcanoes such as Arenal, Poás and Galeras can serve to seal shallow levels of the continental crust, focusing magmatic gas flux towards fumaroles, faults and the fractured lower flanks of the volcanoes. The magmatic gas distributions and isotopic values can be quite variable, due either to heterogeneous permeability within a volcanic edifice or to groundwater transport. Paradoxically, volcanoes responsible for significant output of magmatic gas through the central conduit also act as barriers to gas flow on their upper flanks. We envisage a concentric zoning of gas flow (Fig. 8): an inner zone in the active crater where strong degassing occurs; an intermediate zone on the upper flanks where gas flow is impeded; and an outer, fractured zone where magmatic gas can again reach the surface.

We recommend that the networks covering the three volcanoes be increased and augmented by additional stations in order to better control the gas flux

through the flanks. We suggest that future work incorporate extensive ^{14}C measurements of CO_2 in order to better constrain the magmatic component of the diffuse soil gas.

Appendix: The effect of humidity on radon measurements

Humidity levels within our PVC tubes were probably high. Recently there has been some concern expressed regarding the accuracy and precision of the E-PERM technique under high-humidity conditions. This concern stems from a report by Hopper et al. (1995) in which several types of radon detectors were subjected to different climatic conditions over a period of 90 days. Under high-temperature, high-humidity conditions, the E-PERM devices significantly overestimated the radon concentrations present during the tests.

We took a closer look at these data. Additionally, we made independent laboratory evaluations to assess whether high humidity may affect our E-PERM technique. Our comments (a) address the Hopper et al. (1995) data, (b) examine our use of duplicate E-PERM detectors in PVC tubes, (c) discuss our new laboratory data and (d) discuss the E-PERM technique of measuring radon in water. These four points bear directly on the problem of high humidity.

Hopper et al. (1995) showed that the E-PERM technique overestimated radon concentrations under high-temperature and high-humidity conditions (35–40 °C, 85–95 % RH). Furthermore, the results were highly variable from one detector to the next. It is important to note that the exposure period was 90 days. As a result of the humidity and long exposure, fungus was able to grow on the E-PERM detectors, contrary to what was reported by Hopper et al. (1995) (P. Kotrappa, pers. commun. 1996). The presence of fungus probably compromised the voltage readings of the detectors, resulting in variable false-positive readings.

Table 3 Comparison of Electret voltage changes during dry and humid conditions

| Jar No. | Temperature (°C) | Relative Humidity (%) | Electret No. | Delta Time (days) | Initial Volts | Final Volts | Delta Volts |
|---------|------------------|-----------------------|--------------|-------------------|---------------|-------------|-------------|
| 5 | 20–22 | 23–24 | SQ8270 | 18.8854 | 455 | 413 | 42 |
| 6 | 20–22 | 23–24 | SQ831 1 | 18.8847 | 501 | 458 | 43 |
| 7 | 20–22 | 23–24 | SP0238 | 18.8847 | 499 | 453 | 46 |
| 8 | 20–22 | 100 | SP0219 | 18.8833 | 444 | 400 | 44 |
| 9 | 20–22 | 100 | SP0242 | 18.8826 | 436 | 391 | 45 |

Volume of jar is 3.74 l. Electret configuration: standard chamber with short-term blue electret. All voltage measurements made at 24 °C

By contrast with the foregoing data and results, the exposure period for our field measurements was always 1 week or less. Mold or fungus was never observed on the detectors. We generally analysed duplicate detectors in each PVC tube, one detector at the top of the tube and the other at the bottom. Despite the likelihood of temperature and humidity gradients between the top and bottom of the tube, the two detectors gave results within 10 % of each other.

To further investigate the problem of high humidity, we conducted laboratory measurements of radon under controlled conditions. We measured a combination of radon concentrations and the gamma background in sealed glass jars over a period of 19 days. Temperature was maintained at 20–22 °C, whereas relative humidity was 23–24 % for three analyses and 100 % for two other analyses (Table 3). No mold or fungus was observed on the detectors after the exposure period. Voltage changes of the detectors were compared for the low-humidity (average 43.7 volts) and high humidity (average 44.5 volts) conditions. The difference between these averages is 2 %, and we conclude there was no discernible difference in detector performance under vastly different humidity conditions.

As a final point, the E-PERM method commonly is used to measure radon concentrations in water. This is done by placing the water sample and radon detectors in a sealed glass jar, similar to our experiment discussed previously. This sealing process effectively results in 100 % humidity conditions within the jar. The E-PERM results have been traced to NIST calibration standards with excellent results (Collé et al. 1995). This is additional evidence that E-PERM measurements under high-humidity conditions are both accurate and precise, provided the exposure time is not too long to prevent growth of mold and fungus on the detector surfaces.

Acknowledgements We are grateful to E. Malavassi and all the staff of OVSICORI for their enthusiastic support, as well as the personnel of the Poás and Arenal National Parks for allowing us access to the volcanoes. We also greatly appreciate the support of INGEOMINAS in Pasto, Colombia. We thank A. E. Williams-Jones for constructive criticism and support. The research was supported by grants to J.S. from the Natural Sciences and Engineering Research Council of Canada, the “Fonds pour la Formation de Chercheurs et l’Aide à la Recherche” (Québec),

and the Université de Montréal. Careful reviews by D. Thomas, W.C. Evans and C. Newhall greatly improved this work.

References

- Allard P (1998) Magma-derived CO₂ budget of Mount Etna. *EOS Trans Am Geophys Union* 79:F927
- Allard P, Carbonnelle J, Dajlevic D, Le Bronec J, Morel P, Robe MC, Maurenas JM, Faivre-Pierret R, Martin D (1991) Eruptive and diffuse emissions of CO₂ from Mount Etna. *Nature* 351:387–391
- Badalamenti B, Gangi F di, Guerrieri S, Valenza M (1993) Continuous monitoring (temperature, CO₂ in soil gases and reducing capacity). *Acta Volcanol* 3:269–271
- Barberi F, Carapezza ML (1994) Helium and CO₂ soil gas emissions from Santorini (Greece). *Bull Volcanol* 56:335–342
- Baubron J-C, Allard P, Sabroux J-C, Tedesco D, Toutain J-P (1991) Soil gas emanations as precursory indicators of volcanic eruptions. *J Geol Soc Lond* 148:571–576
- Borgia A, Poore C, Carr MJ, Melson WG, Alvarado GE (1988) Structural, stratigraphic, and petrographic aspects of the Arenal-Chato volcanic system, Costa Rica: evolution of a young stratovolcanic province. *Bull Volcanol* 50:86–105
- Brantley SL, Koepenick KW (1995) Measured carbon dioxide emissions from Oldoinyo Lengai and the skewed distribution of passive volcanic fluxes. *Geology* 23:933–936
- Calvache ML, Cortés GP, Williams SN (1997) Stratigraphy and chronology of Galeras Volcanic Complex, Colombia. *J Volcanol Geotherm Res* 77:5–19
- Charland A, Stix J, Barquero J, Fernandez E (1994) Radon and CO₂ soil degassing at Poás Volcano, Costa Rica: preliminary results. *EOS Trans Am Geophys Union* 75:717
- Collé R, Kotrappa P, Hutchinson JMR (1995) Calibration of electret-based integral radon monitors using NIST polyethylene-encapsulated ²²⁶Rn/²²²Rn emanation (PERE) standards. *J Res Natl Inst Stand Technol* 100:629–639
- Connor C, Hill B, LaFemina P, Navarro M, Conway M (1996) Soil ²²²Rn pulse during the initial phase of the June to August 1995 eruption of Cerro Negro, Nicaragua. *J Volcanol Geotherm Res* 73:119–127
- Crenshaw WB, Williams SN, Stoiber RE (1982) Fault location by radon and mercury detection at an active volcano in Nicaragua. *Nature* 300:345–346
- D’Alessandro W, Giammanco S, Parello F, Valenza M (1997) CO₂ output and δ¹³C(CO₂) from Mount Etna as indicators of degassing of shallow asthenosphere. *Bull Volcanol* 58:455–458
- Dugas WA (1993) Micrometeorological and chamber measurements of CO₂ flux from bare soil. *Agricult Forest Meteorol* 67:115–128
- Farrar CD, Sorey ML, Evans WC, Howle JF, Kerr BD, Kennedy BM, King C-Y, Southon JR (1995) Forest-killing diffuse CO₂ emission at Mammoth Mountain as a sign of magmatic unrest. *Nature* 376:675–678

- Fernandez IJ, Son YW, Kraske CR, Rustad LE, David MB (1993) Soil carbon-dioxide characteristics under different forest types and after harvest. *Soil Sci Soc Am J* 57:1115–1121
- Fischer TP, Sturchio NC, Stix J, Arehart GB, Counce D, Williams SN (1997) The chemical and isotopic composition of fumarolic gases and spring discharges from Galeras Volcano, Colombia. *J Volcanol Geotherm Res* 77:229–253
- Gasparini P, Mantovani MSM (1978) Radon anomalies and volcanic eruptions. *J Volcanol Geotherm Res* 3:325–341
- Gerlach TM, Doukas MP, McGee KA, Kessler R (1998) Three-year decline of magmatic CO₂ emissions from soils of a Mammoth Mountain tree kill: Horseshoe Lake, CA, 1995–1997. *Geophys Res Lett* 25:1947–1950
- Giammanco S, Gurrieri S, Valenza M (1998) Anomalous soil CO₂ degassing in relation to faults and eruptive fissures on Mount Etna (Sicily, Italy). *Bull Volcanol* 60:252–259
- Hall ML, Wood CA (1985) Volcano-tectonic segmentation of the northern Andes. *Geology* 13:203–207
- Heiligmann M (1996) Soil gases at Galeras volcano, Colombia, and their utility in eruption prediction. MSc thesis, Univ Montréal, 114 pp
- Heiligmann M, Stix J, Williams-Jones G, Sherwood Lollar B, Garzón G (1997) Distal degassing of radon and carbon dioxide on Galeras volcano, Colombia. *J Volcanol Geotherm Res* 77:267–283
- Hinkle ME (1990) Factors affecting concentrations of helium and carbon dioxide in soil gases. In: Durance EM (ed) *Geochemistry of gaseous elements and compounds*. Theophrastus Publications SA, Athens, pp 421–447
- Hopper RD, Levy RA, Steinhausler F (1995) IEFA-EPA International climatic test program for integrating radon detectors
- James ER, Manga M, Rose TP (1999) CO₂ degassing Oregon Cascades. *Geology* 27:823–826
- Janssens IA, Barigah ST, Ceulemans R (1998) Soil CO₂ efflux rates in different tropical vegetation types in French Guiana. *Ann Sci Forest* 55:671–680
- King CY (1980) Episodic radon changes in subsurface soil gas along active faults and possible relation to earthquakes. *J Geophys Res* 83:3065–3078
- Koepnick KW, Brantley SL, Thompson JM, Rowe GL, Nyblade AA, Moshy C (1996) Volatile emissions from the crater and flank of Oldoinyo Lengai volcano, Tanzania. *J Geophys Res* 101:13819–13830
- Kotrappa P, Stieff LR (1992) Elevation correction factors for E-PERM radon monitors. *Health Phys* 62:82–86
- Kotrappa P, Dempsey JC, Hickey JR, Stieff LR (1988) An electrode passive environmental ²²²Rn monitor based on ionization measurement. *Health Phys* 54:47–56
- Malavassi E (1979) Geology and petrology of Arenal Volcano, Costa Rica. MSc thesis, Univ Hawaii, 111 pp
- Moore TR, Roulet NT (1991) A comparison of dynamic and static chambers for methane emission measurements from subarctic fens. *Atmosphere Oceans* 29:102–109
- Pinol J, Alcaniz JM, Roda F (1995) Carbon-dioxide efflux and PCO₂ in soils of 3 Quercus-Ilex Montane forests. *Biogeochemistry* 30:191–215
- Prosser JT, Carr MJ (1987) Poás volcano, Costa Rica: geology of the summit region and spatial and temporal variations among the most recent lavas. *J Volcanol Geotherm Res* 33:131–146
- Rad Elec Inc. (1993) E-PERM^R system manual. Rad Elec Inc., Virginia, USA
- Rahn TA, Fessenden JE, Wahlen M (1996) Flux chamber measurements of anomalous CO₂ emission from the flanks of Mammoth Mountain, California. *Geophys Res Lett* 23:1861–1864
- Rose TP, Davisson ML (1996) Radiocarbon in hydrologic systems containing dissolved magmatic carbon dioxide. *Science* 273:1367–1370
- Rowe GL, Brantley SL, Fernandez JF, Borgia A (1995) The chemical and hydrologic structure of Poás Volcano, Costa Rica. *J Volcanol Geotherm Res* 64:233–267
- Schery SD, Petschek AG (1983) Exhalation of radon and thoron: the question of the effect of thermal gradients in soil. *Earth Planet Sci Lett* 64:56–60
- Shapiro MH, Melvin D, Tombrello TA, Whitcomb JH (1980) Automated radon monitoring at a hard rock site in the southern California transverse ranges. *J Geophys Res* 85:3058–3064
- Stix J, Zapata JA, Calvache M, Cortes GP, Gómez D, Narvaez L, Ordoñez M, Ortega A, Torres R, Williams SN (1993) A model of degassing at Galeras Volcano, Colombia, 1988–1993. *Geology* 21:963–967
- Stix J, Torres R, Narváez L, Cortés GP, Raigosa J, Gómez D, Castonguay R (1997) A model of vulcanian eruptions at Galeras volcano, Colombia. *J Volcanol Geotherm Res* 77:285–303
- Stoiber RE, Carr MJ (1973) Quaternary volcanic and tectonic segmentation of Central America. *Bull Volcanol* 37:304–325
- Thomas DM, Cuff KE, Cox ME (1986) The association between ground gas radon variations and geologic activity in Hawaii. *J Geophys Res* 91:12186–12198
- Williams-Jones G, Heiligmann M, Charland A, Sherwood Lollar B, Stix J (1997) A model of diffuse degassing at three subduction-related volcanoes. IAVCEI General Assembly:65